

**EXPERIMENTAL VALIDATION OF FLEXIBLE ROBOT
ARM MODELING AND CONTROL**

OUTLINE

- **INTRODUCTION**
Motivation
Background
- **MODEL EVALUATION**
Formulation
Results
- **CONTROLLER EVALUATION**
Formulation
Results
- **SUMMARY AND CONCLUSIONS**

M

A. Galip Ulsoy

**Mechanical Engineering and Applied Mechanics
College of Engineering
University of Michigan**

INTRODUCTION

- Flexibility is important for high speed, high precision operation of lightweight manipulators.
- Accurate dynamic modeling of flexible robot arms is needed. Previous work has mostly been based on linear elasticity with prescribed rigid body motions (i.e., no effect of flexible motion on rigid body motion).
- Little or no experimental validation of dynamic models for flexible arms is available. Experimental results are also limited for flexible arm control.
- We include the effects of prismatic as well as revolute joints.
- We investigate the effect of full coupling between the rigid and flexible motions, and of axial shortening.
- We also consider the control of flexible arms using only additional sensors.

BACKGROUND

Research since 1970's

(e.g., [Book, Maizzo-Neto, Whitney 75])

Modeling of flexible mechanisms and structures

(e.g., Elasto-Kineto Dynamics, Floating Frames, 70's)

Approaches to control

Trajectory planning [Meckl, Seering 83,85]

Open loop (none)

Closed loop with micromanipulator

[Cannon et al, Book et al]

Closed loop with additional sensors only (none)

Experimental work

[Zalucky and Hardt 84]

[Cannon et al 83, 84]

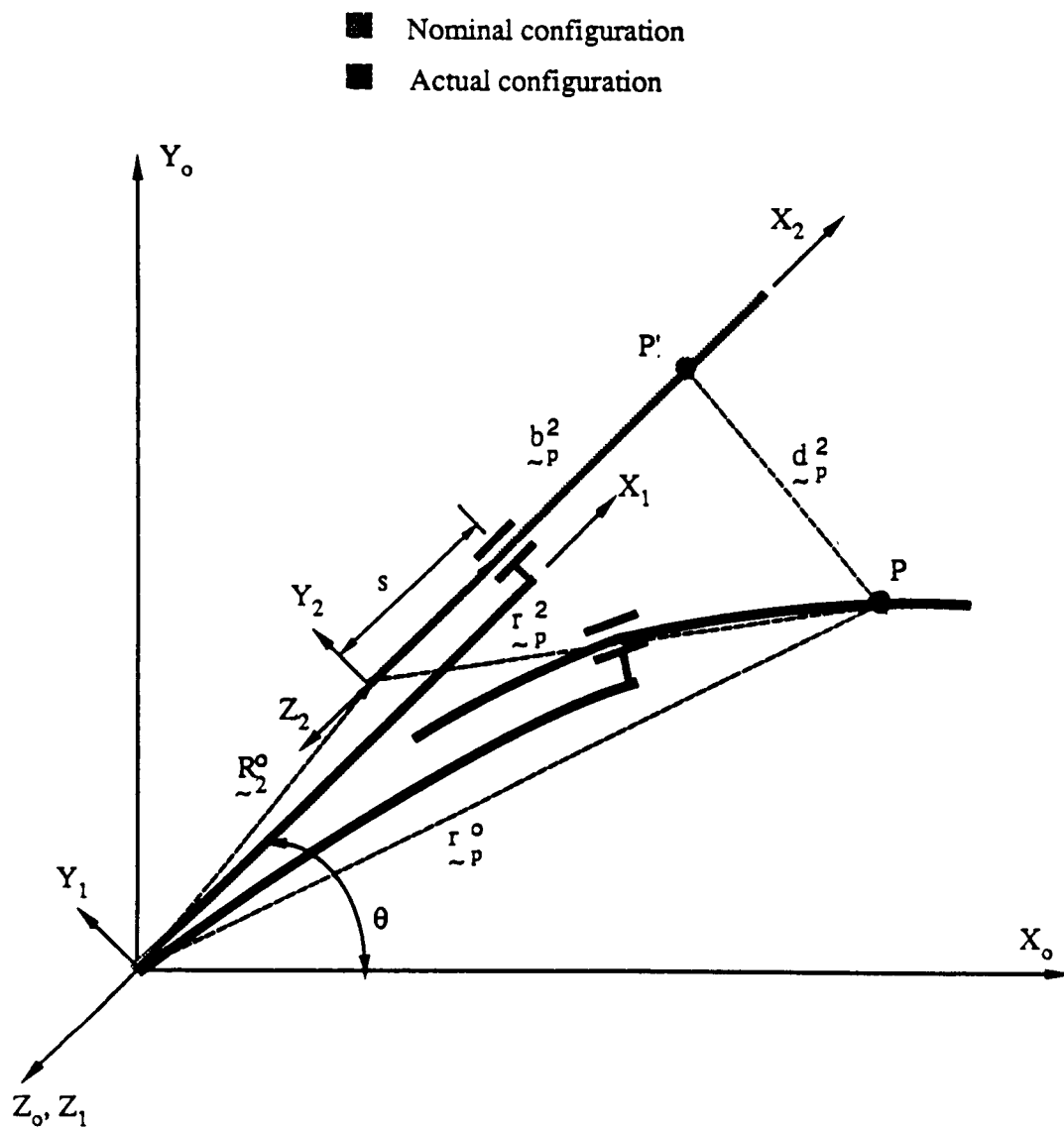
Theoretical control studies

[Book et al, Cannon et al, etc, early 1980's]

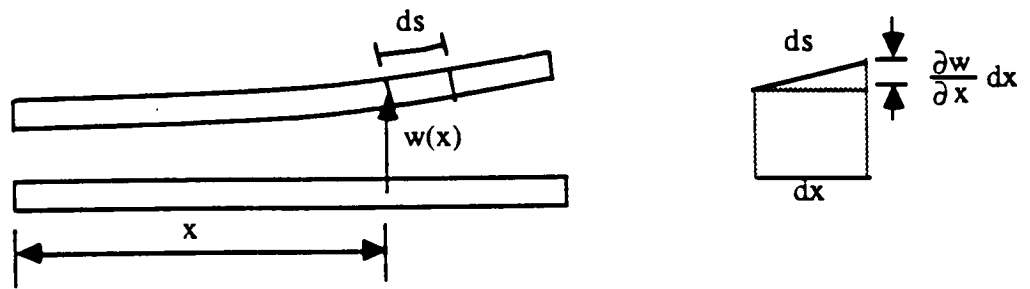
Various control strategies proposed typically assuming all states available, no spillover, simple models, no implementation considerations.

MODELING AND SIMULATION OF FLEXIBLE ROBOTS WITH PRISMATIC JOINTS

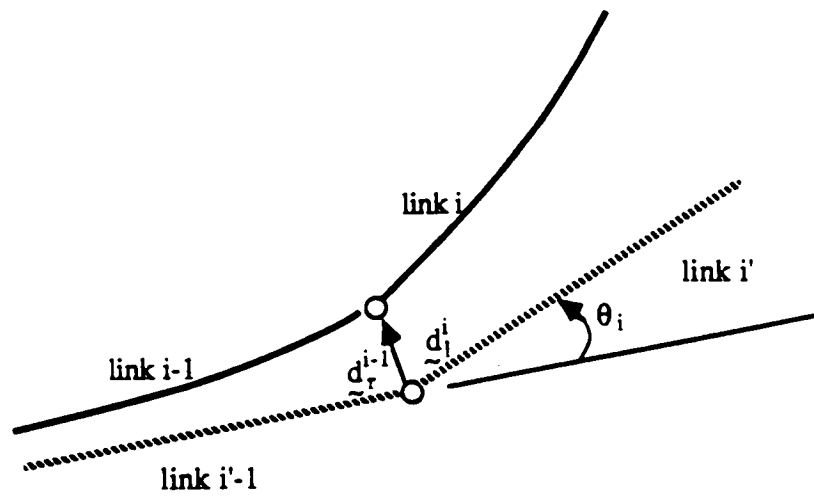
- **Robots with both rigid and flexible links attached with revolute and/or prismatic joints can be modeled and analyzed.**
- **The equations of motion are derived using Lagrange's equations. The prescribed motion, and prescribed torque/force cases can both be handled.**
- **Flexible elements are represented as Euler-Bernoulli beams, and the axial shortening effect is also included.**
- **Finite element analysis is used for the discretization of the resulting hybrid equations of motion.**
- **Constraints are handled using Lagrange multipliers.**
- **The resulting algebraic-differential equations are solved numerically using constraint stabilization methods.**



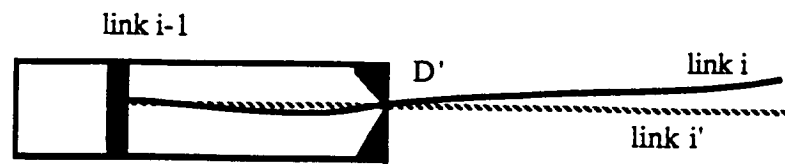
Schematic of a two-link robot.



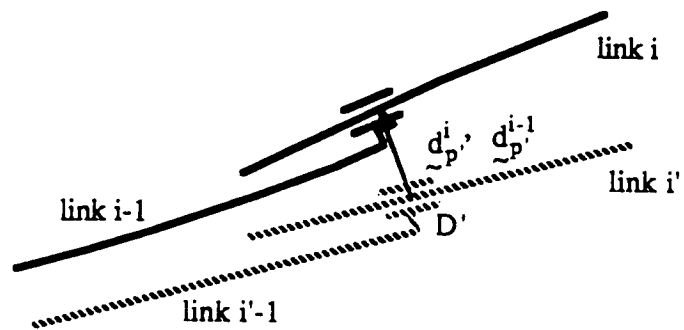
Axial shortening of a beam under plane transverse deflection.



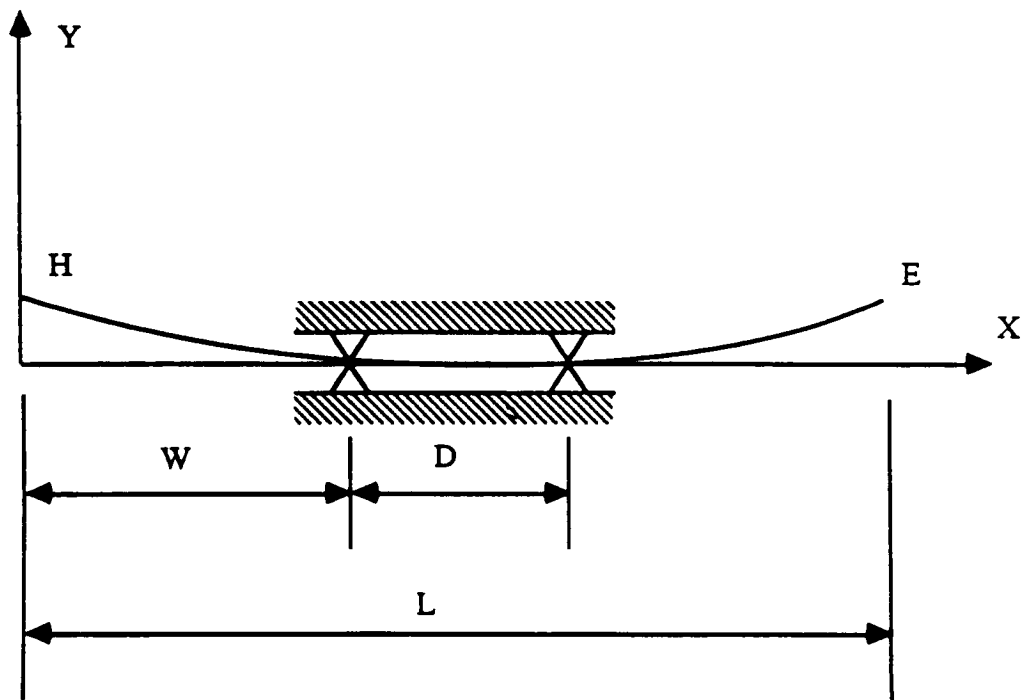
Schematic of revolute joint i .



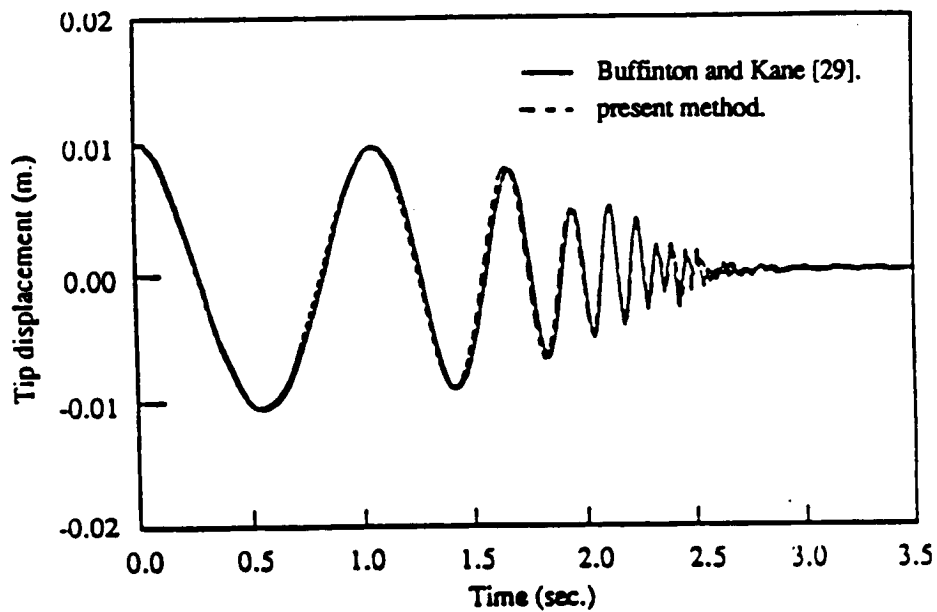
Schematic of prismatic joint i .



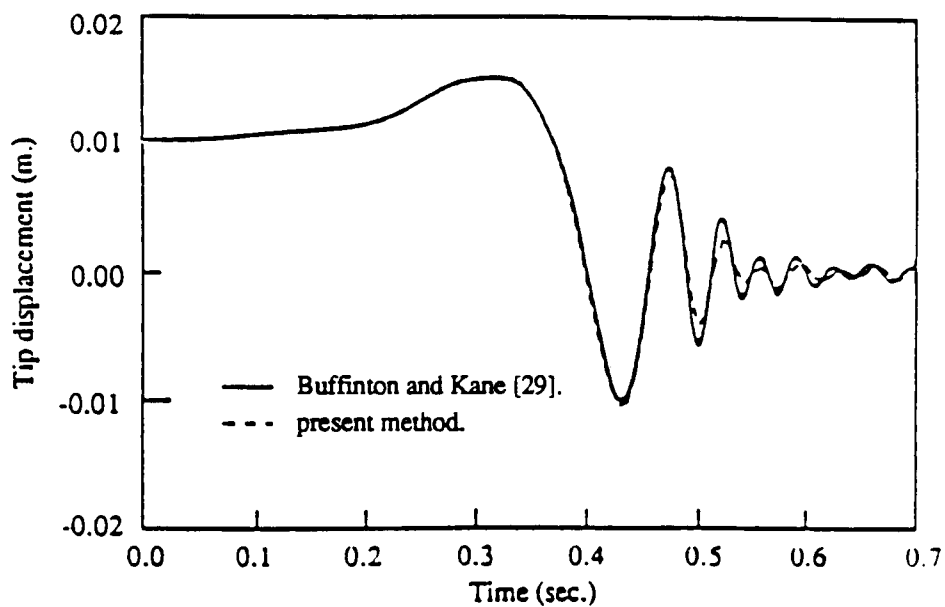
Schematic of prismatic joint i .



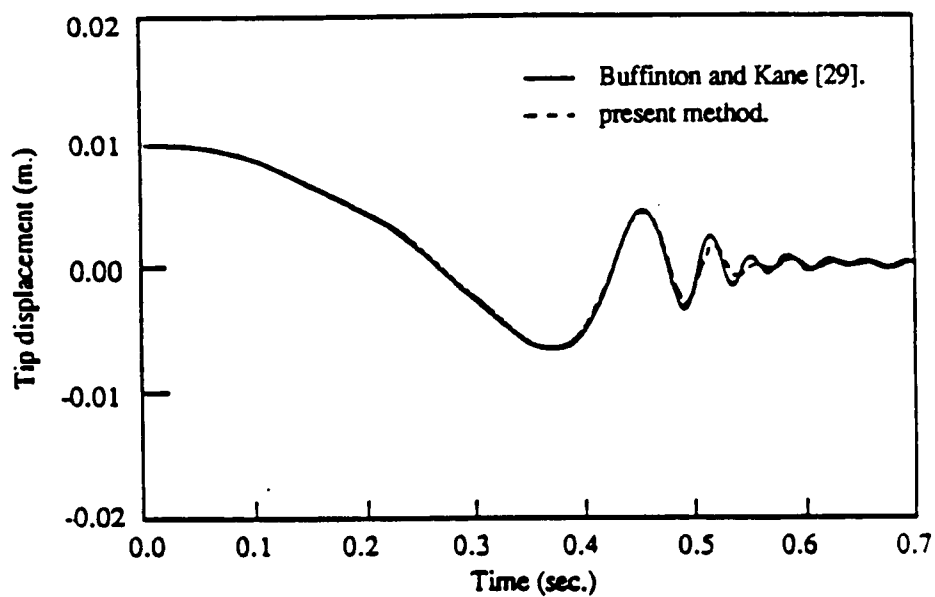
Beam moving over bilateral supports.



Tip displacement in "slow push" case with $C_1 = 0.725$ m, $C_2 = 0.7$ m and $T = 3.5$ sec.



Tip displacement in "fast push" case with
 $C_1 = 0.725$ m, $C_2 = 0.7$ m and $T = 0.7$ sec.



Tip displacement in "fast pull" case with
 $C_1 = 0.025$ m, $C_2 = -0.7$ m and $T = 0.7$ sec.

LABORATORY ROBOT

Small table top spherical coordinate robot with 3 DOF

Designed and built at UM

Interfaced to an IBM PC/XT

Convenient test bed experimental research work

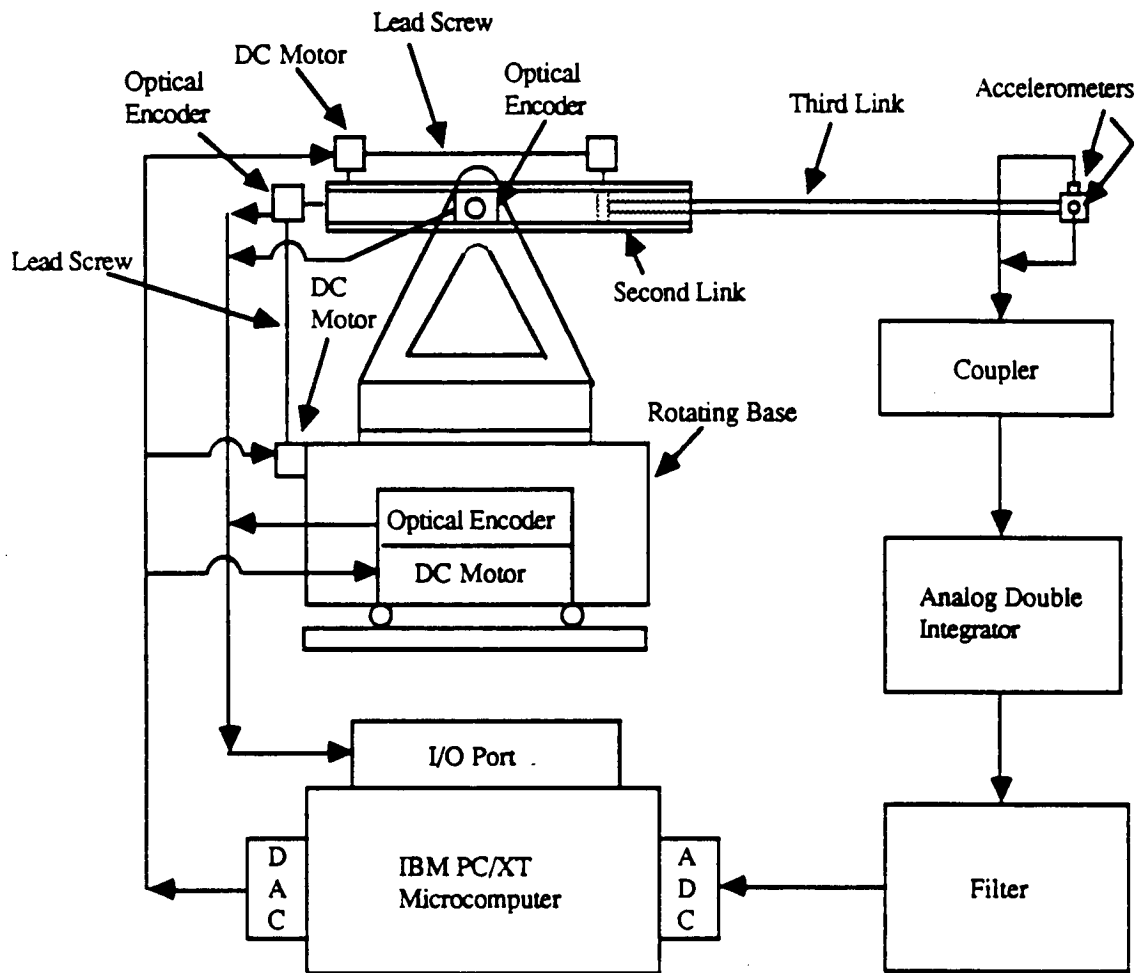
r and θ axes are dc motor driven through leadscrews

ϕ axis is dc motor driven through a gear train

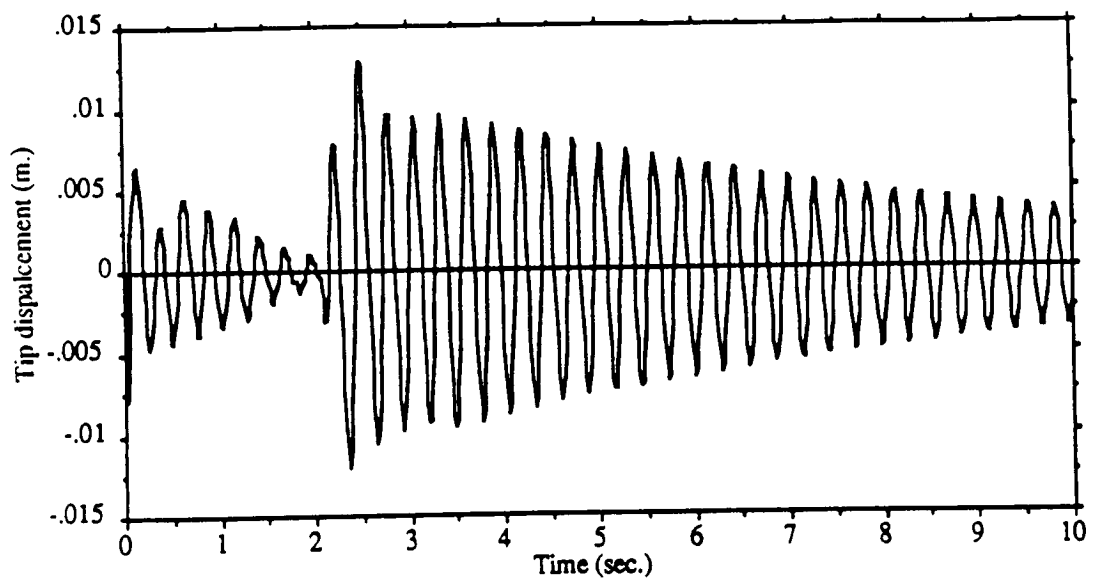
all axes have tachometers and optical incremental encoders with counter circuits

last link is intentionally designed to be flexible

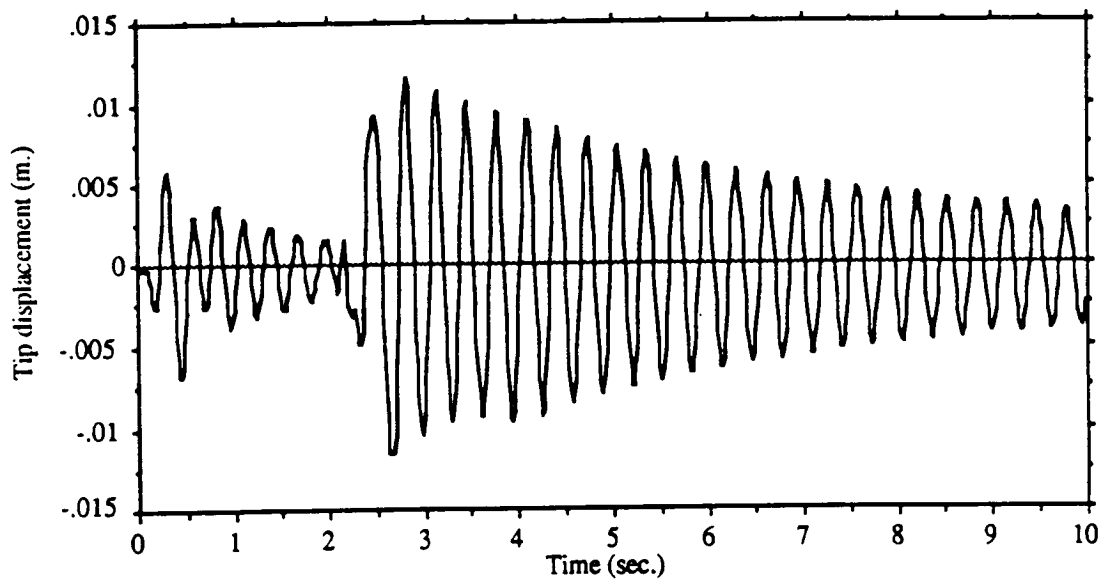
**accelerometers (in two orthogonal directions)
measure end of arm accelerations which are
integrated to get velocities and positions**



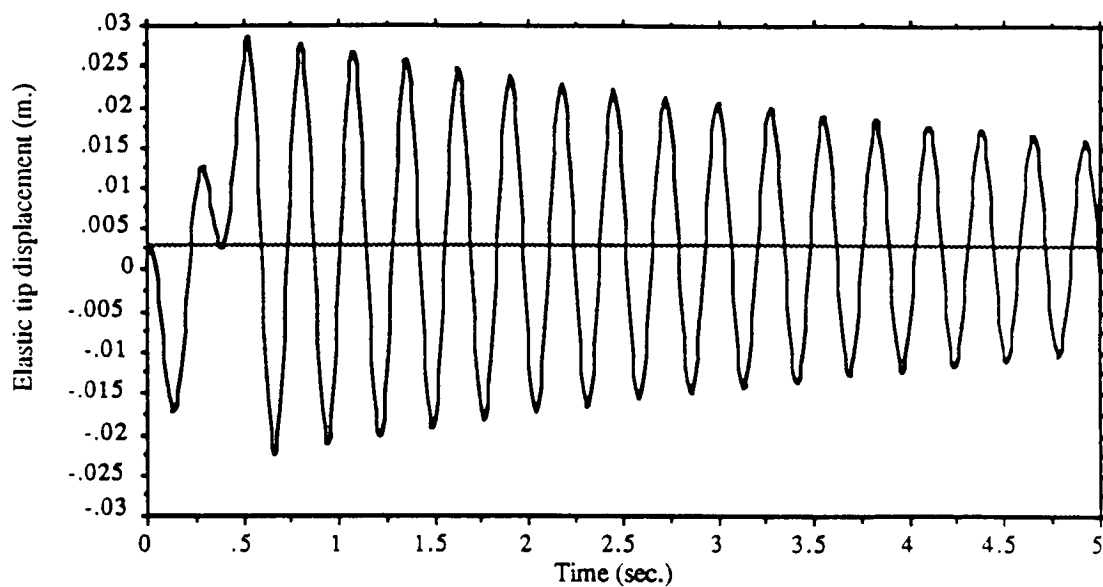
Schematic of the experimental setup.



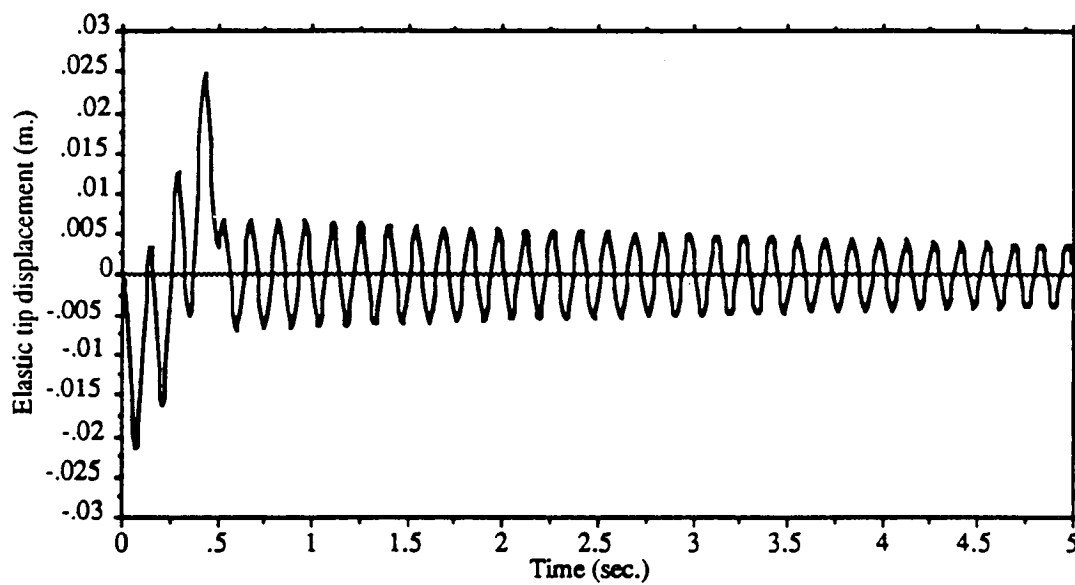
Elastic tip displacement obtained by numerical simulation after filtering.



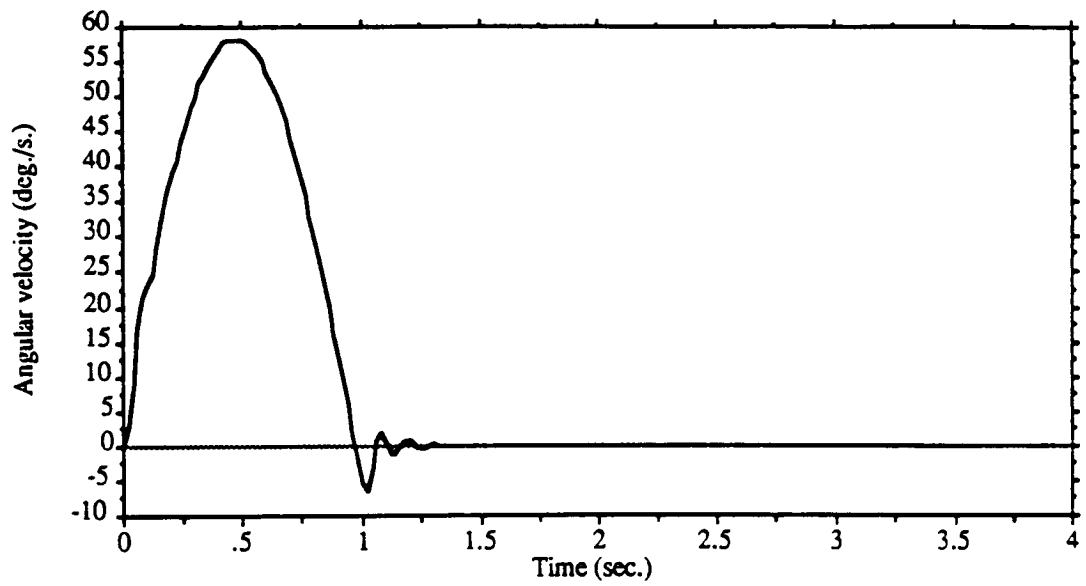
Vertical elastic tip displacement of the last link in the two-dimensional maneuver.



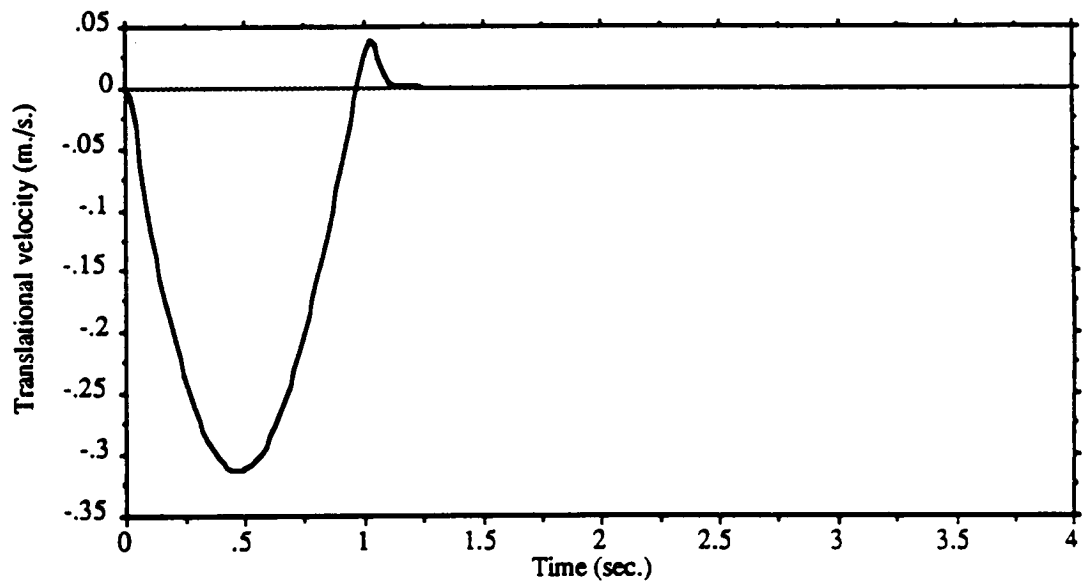
The elastic tip displacement obtained from the equations of motion with prescribed motions.



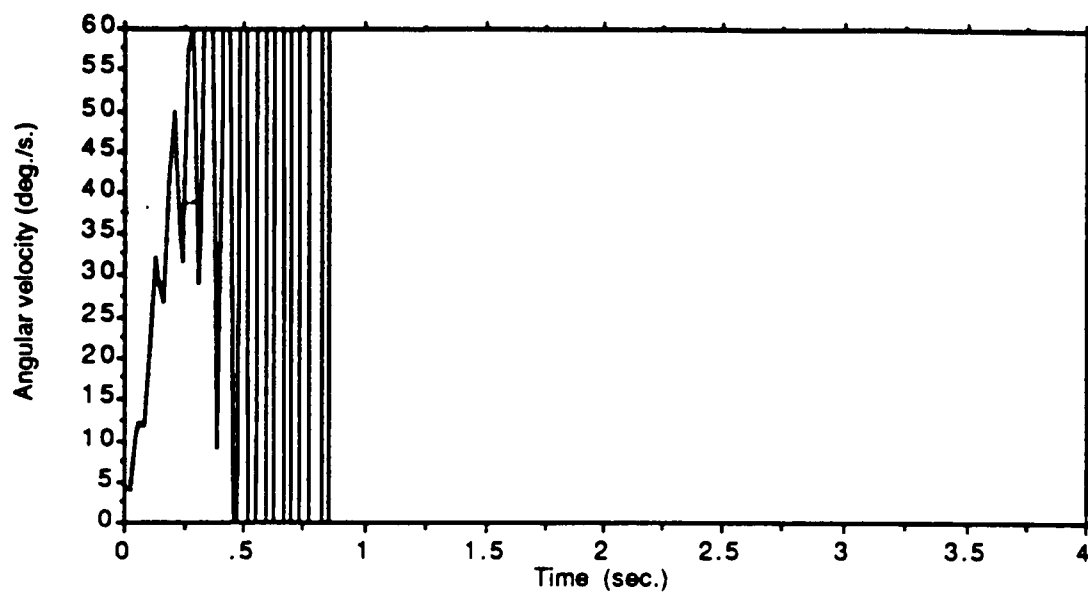
Elastic tip displacement obtained from the equations of motion with prescribed torque/force.



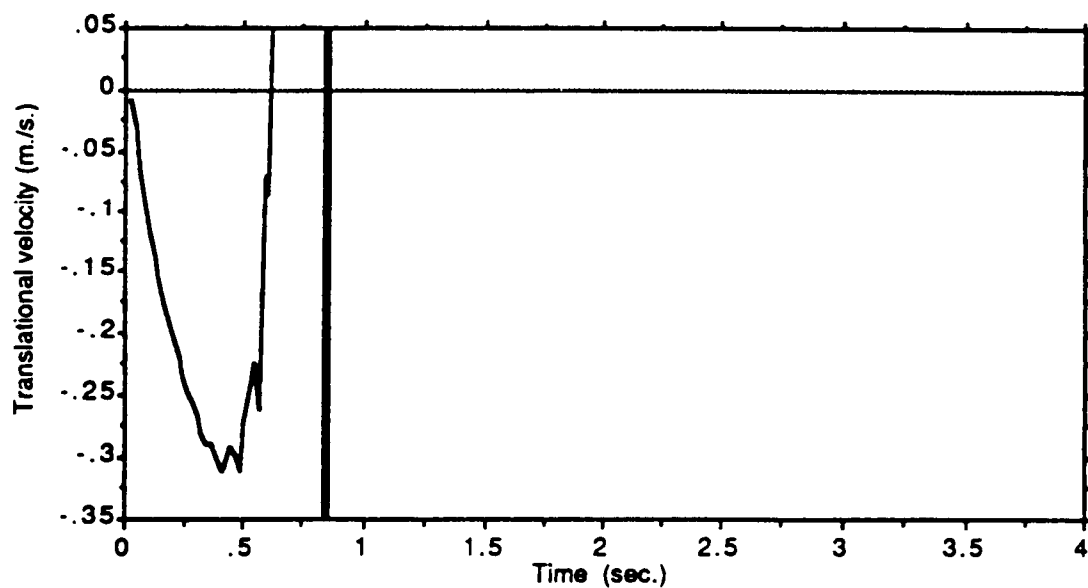
Angular velocity of the first joint of the rigid manipulator with controller.



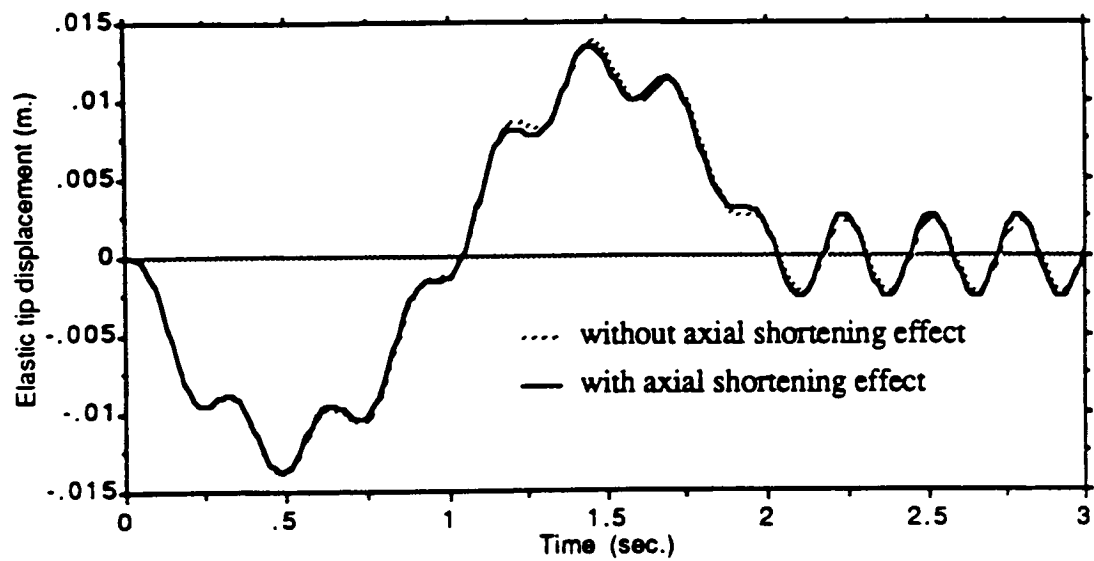
Translational velocity of the third joint of the rigid manipulator with controller.



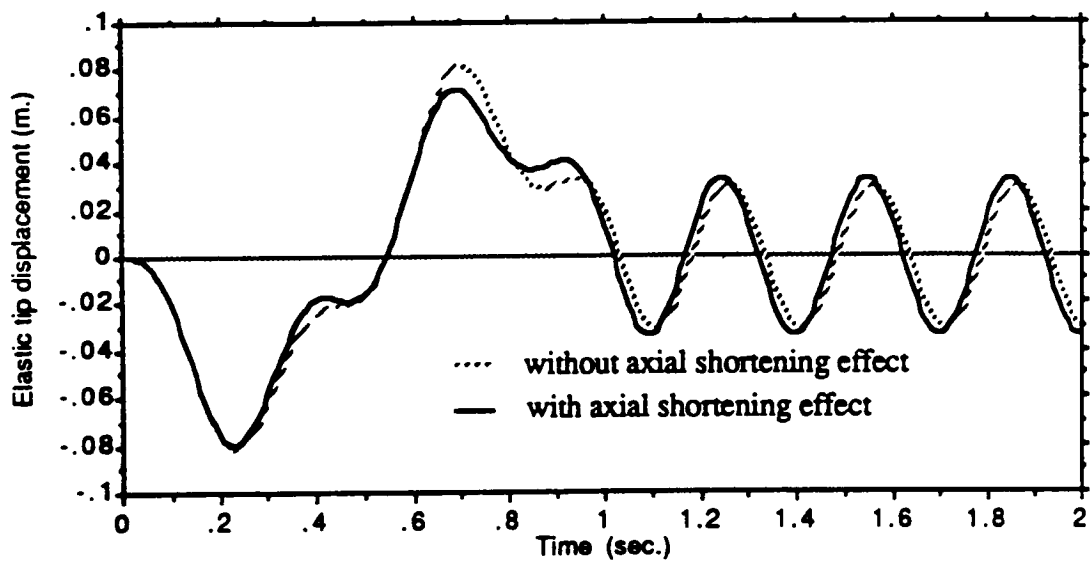
Angular velocity of the first joint of the flexible manipulator with controller.



Translational velocity of the third joint of the flexible manipulator with controller.



Elastic tip displacements in the case with $T = 2$ sec.



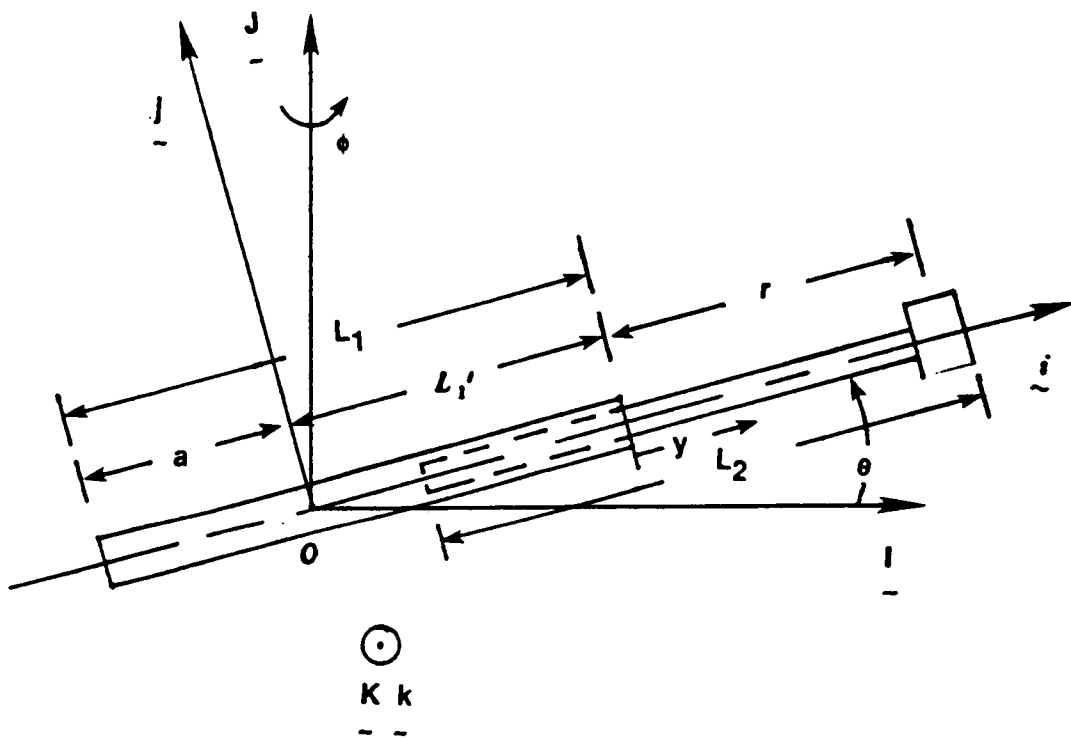
Elastic tip displacement in the case with $T = 1$ sec.

SUMMARY AND CONCLUSIONS

- **A general modeling procedure for robot arms consisting of rigid and flexible links connected by revolute and/or prismatic joints has been developed and experimentally validated.**
- **The significance of full coupling (effect of flexible motion on rigid body motion) has been demonstrated.**
- **The axial shortening effect is shown to be significant for high speed operation of lightweight manipulators.**

CONTROL OF A LEADSCREW DRIVEN FLEXIBLE ROBOT ARM

- **The laboratory robot is used to compare the performance of a rigid body motion controller with that of a rigid and flexible motion controller.**
- **The rigid body motion controller uses only the joint motion measurements and joint actuators. The rigid and flexible motion controller also uses the end of arm motion measurements, but no additional actuators.**
- **The leadscrew transmission characteristics as well as observation and control spillover are considered.**
- **The numerical and experimental results show good agreement, and indicate that significant reductions in arm vibration are possible through use of the rigid and flexible motion controller.**



Arm geometry and coordinates.

PHYSICAL CONSTRAINTS

The physical constraints that are considered in this work are the ones imposed by the leadscrews only.

- . Condition for self locking assumption to be valid is:**

$$\mu > \tan(\psi_1)$$

where

μ is the thread coefficient of friction.

ψ_1 is the thread helix angle.

- . Effect of the self locking condition.**
- . Effect of coulomb friction.**

CONTROLLER DESIGN

Equations of motion:

$$\underline{M}(\underline{x}) \underline{\ddot{x}} + \underline{F}(\underline{x}, \underline{\dot{x}}) = \underline{F}'(\underline{I})$$

$$\underline{x}^T = [r, \theta, \phi, q_{11}, q_{12}, q_{21}, q_{22}]$$

$$\underline{I}^T = [\tau_1, \tau_2, \tau_3]$$

Linearized equations:

$$\underline{\dot{y}} = \underline{A} \underline{y} + \underline{B} \underline{u}$$

$$\underline{y}^T = [\delta \underline{x}^T \ \delta \underline{\dot{x}}^T] ; \quad \underline{u} = \delta \underline{I}$$

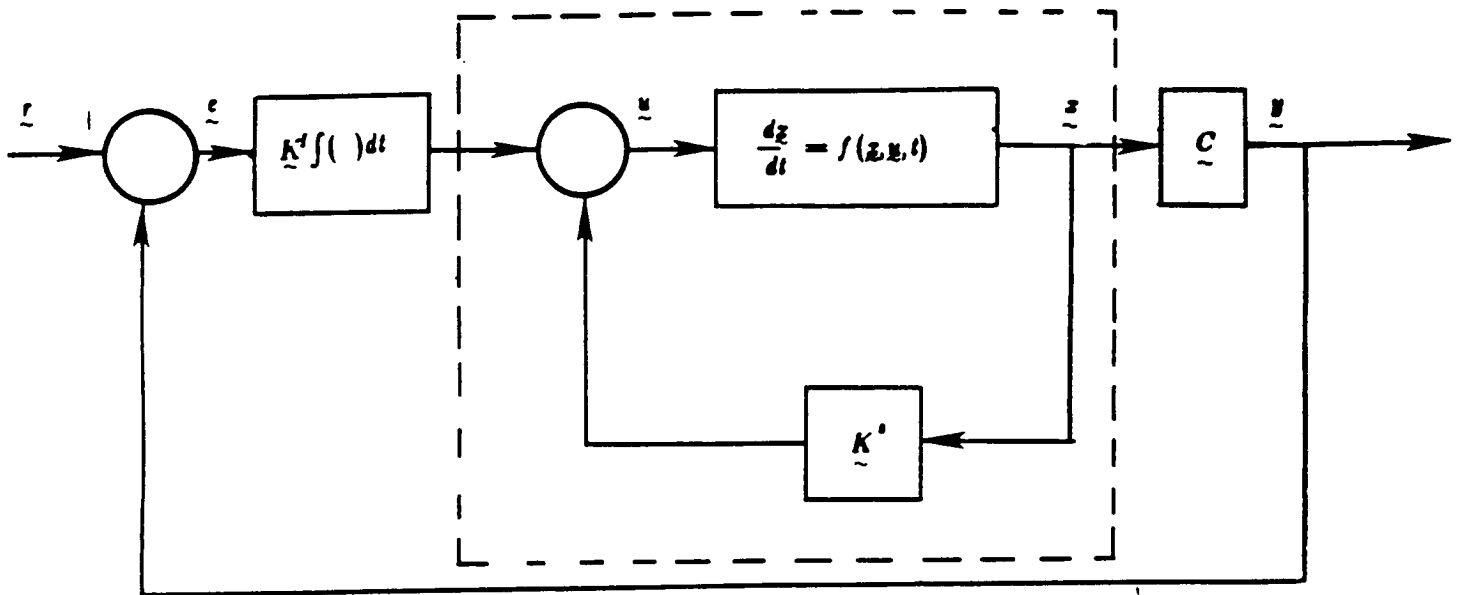
$$\delta \underline{x}^T = [\delta r, \delta \theta, \delta \phi, \delta q_{11}, \delta q_{21}]$$

Integral plus state feedback controller:

$$y_{11} = \int_0^t (y_1 - R_1) dt ; \quad y_{12} = \int_0^t (y_2 - R_2) dt ; \quad y_{13} = \int_0^t (y_3 - R_3) dt$$

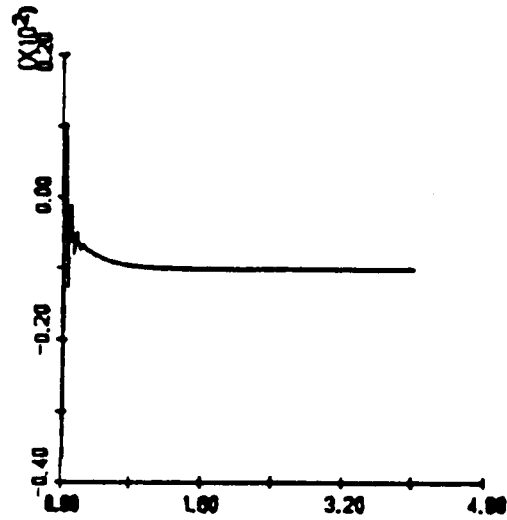
$$\underline{u} = -\underline{K}^F \underline{y}$$

$$\underline{\dot{y}} = (\underline{A} - \underline{B}\underline{K}^F) \underline{y}$$



Block diagram of the Integral plus state feedback controller.

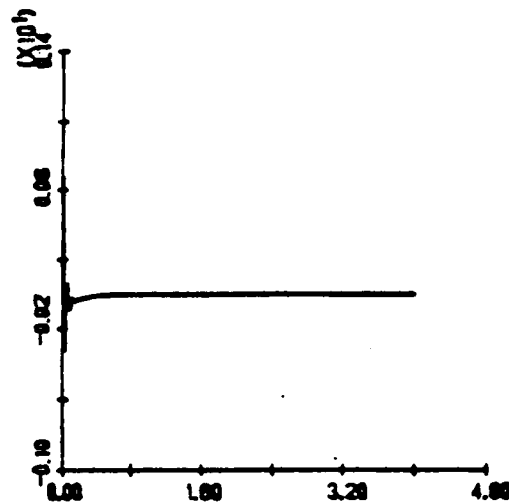
Displacement
 $q_{11}(t)$ (meter)



Time, t (second)

Figure 3. Flexible motion coordinate, $q_{11}(t)$, in response to the rigid and flexible motion controller in the reduced order model case.

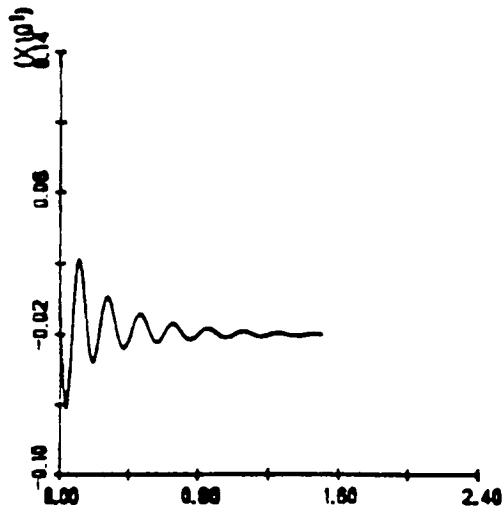
Displacement
 $q_{21}(t)$ (meter)



Time, t (second)

Figure 4. Flexible motion coordinate, $q_{21}(t)$, in response to the rigid and flexible motion controller in the reduced order model case.

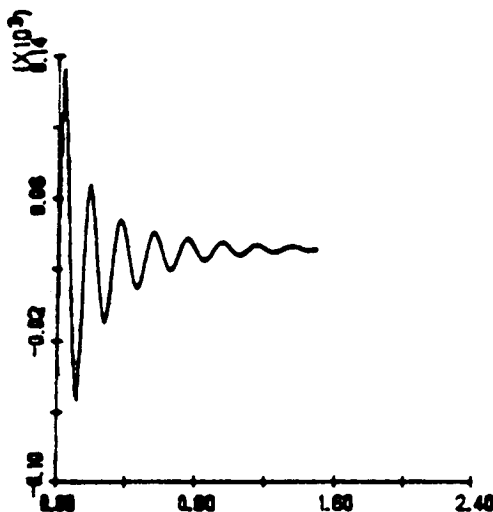
Displacement
 $q_{11}(t)$ (meter)



Time, t (second)

Figure 5. Flexible motion coordinate, $q_{11}(t)$, in response to the rigid and flexible motion controller in the control spillover case.

Displacement
 $q_{12}(t)$ (meter)



Time, t (second)

Figure 6. Flexible motion coordinate, $q_{12}(t)$, in response to the rigid and flexible motion controller in the control spillover case.

ORIGINAL PAGE IS
OF POOR QUALITY

Displacement
 $q_{12}(t)$ (meters)

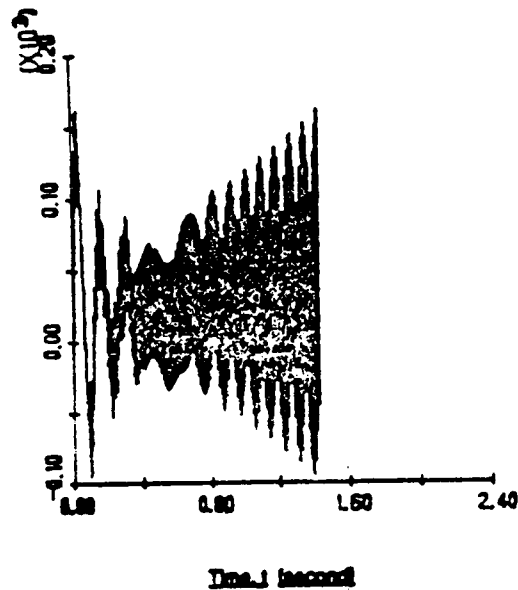


Figure 7. Flexible motion coordinate, $q_{12}(t)$, in response to the rigid and flexible motion controller in the control and observation spillover case.

Displacement
 $q_{12}(t)$ (meters)

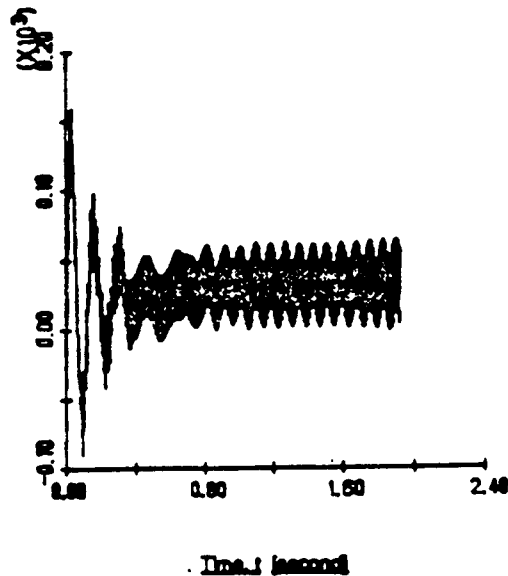


Figure 8. Flexible motion coordinate, $q_{12}(t)$, in response to the rigid and flexible motion controller in the control and observation spillover with structural damping included.

Standard Set of Physical System Parameters	VALUE
Mass of the first beam (m_1)	0.454 Kg
Mass of the second beam (m_2)	0.816 Kg
Mass of the Payload (m_p)	0.07 Kg
Cross sectional area of the second beam (A_2)	0.000151 m ²
Length of the first beam (L_1)	0.233 m
Length of the second beam (L_2)	2 m
Gravitational acceleration (g)	9.81 m/sec ²
Aluminum density (ρ)	2707 Kg/m ³
Flexural rigidity (EI)	770.87 Pa
Reference position for r	1.85 m
Reference position for θ	0 rad
Reference position for ϕ	0 rad
Desired reference position for r	2m
Desired reference position for θ	0.5 rad
Desired reference position for ϕ	0.5 rad
Servo natural frequency for r (ω_{nr})	4 rad/sec
Servo natural frequency for θ ($\omega_{n\theta}$)	4 rad/sec
Servo natural frequency for ϕ ($\omega_{n\phi}$)	8 rad/sec
Flexible motion gain, K_{10}^F	-0.000178
Flexible motion gain, K_{20}^F	-0.084
Flexible motion gain, K_{310}^F	1.568

TABLE 1

	settling time (seconds)	maximum deflection (peak to peak)
rigid body controller	11.0	7.5mm
rigid and flexible motion controller	3.0	2.7mm

Table 2.

ORIGINAL PAGE IS
OF POOR QUALITY

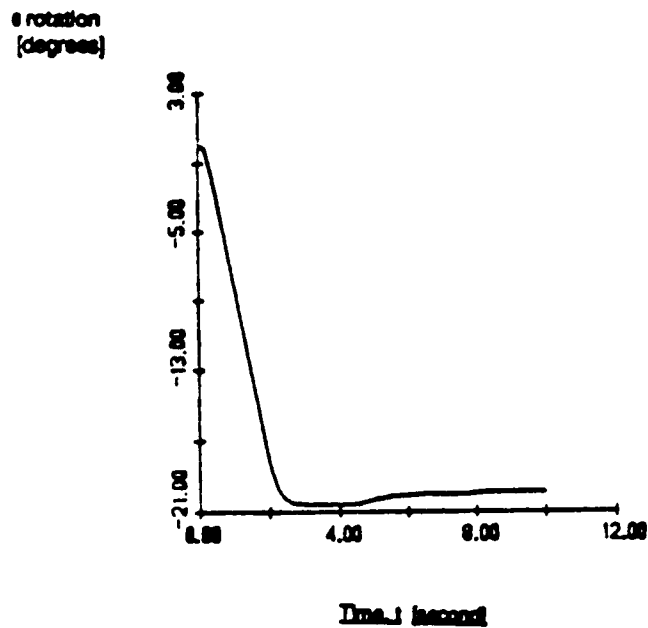


Figure 10. θ response obtained from the rigid body controller in the experimental work.

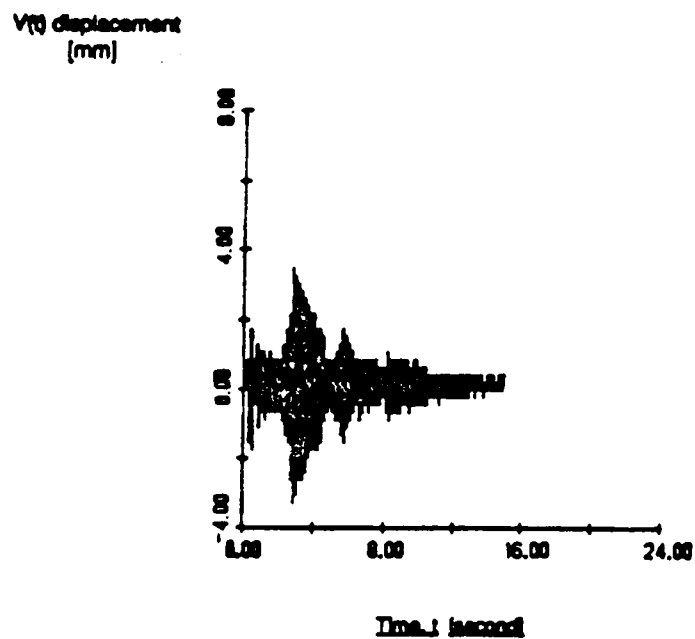


Figure 11. Total vertical deflection in response to the rigid body controller in the experimental work.

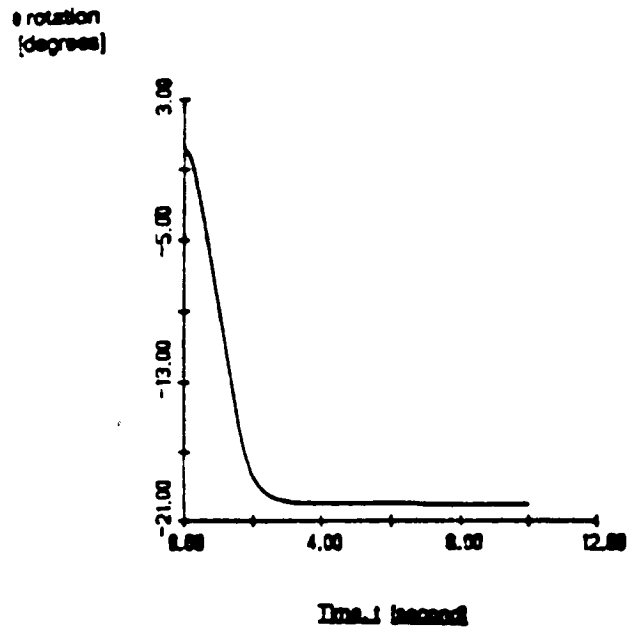


Figure 12. θ response obtained from the rigid and flexible motion controller in the experimental work.

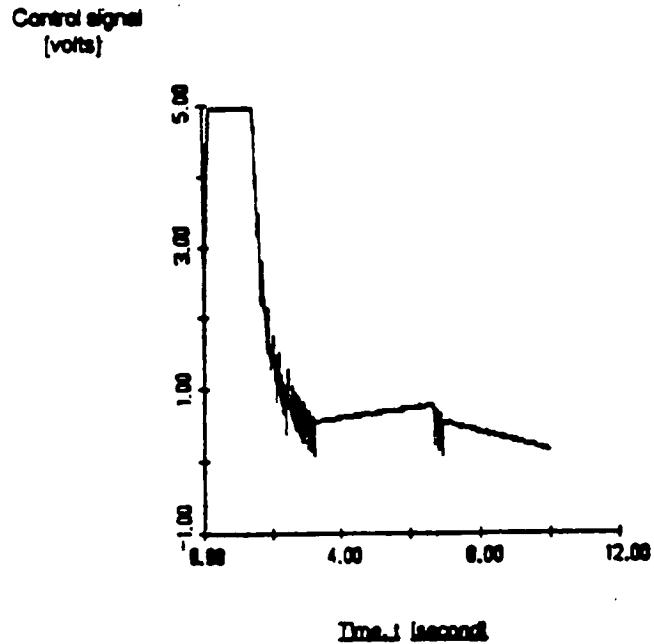


Figure 13. Control signal for the second joint obtained from the rigid and flexible motion controller in the experimental work.

ORIGINAL PAGE IS
OF POOR QUALITY

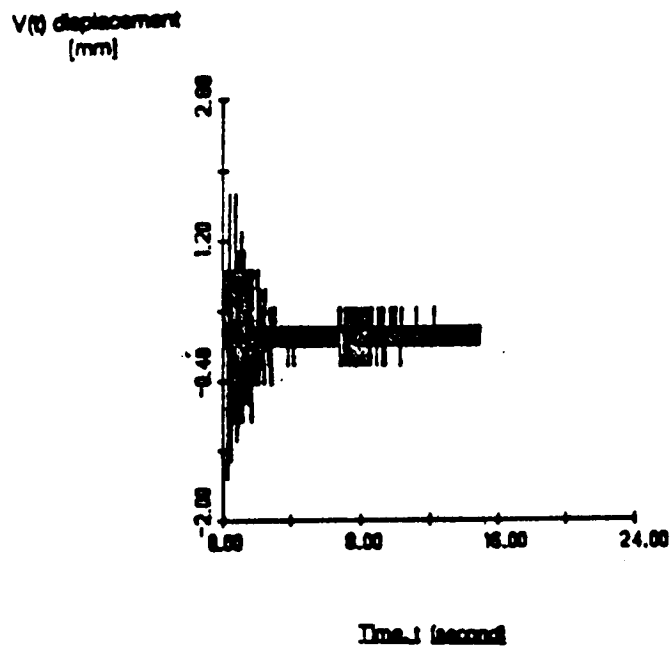


Figure 14. Total vertical deflection in response to the rigid and flexible motion controller in the experimental work.

RIGID BODY CONTROLLER VERSUS RIGID AND FLEXIBLE MOTION CONTROLLER

Simulation results:

- * Control spillover effect can be observed, but does not cause significant deterioration.**
- * Control and observation spillover can destabilize the residual mode. However, a small amount of damping (0.0145) eliminates the problem.**
- * Settling time is reduced from 3.5 to 1.07 seconds, and maximum vibration amplitude is reduced by 50%.**

Experimental results:

- * With low pass filtering and light structural damping, no detrimental spillover effects were observed.**
- * Settling time is reduced from 11 to 3 seconds, and maximum vibration amplitude is reduced by 75%.**

SUMMARY AND CONCLUSIONS

- 1. A dynamic model of a spherical coordinate robot arm, whose last link is flexible, is developed. The constraints imposed by the leadscrew transmission mechanisms are also considered.**
- 2. The interrelationships between the robot arm structural flexibility and the controller design are investigated using a rigid body controller.**
- 3. The rigid and flexible motion controller, which employs additional sensors only, has led to an approximate 50% reduction in the magnitude of the flexible motion even in the presence of the observation and control spillover.**
- 4. The experimental results of the rigid and flexible motion controller show good agreement with those of the digital simulation.**

SUMMARY AND CONCLUSIONS

- **A general modeling method for robot arms with flexible and rigid links connected by prismatic and revolute joints has been presented and experimentally validated.**
- **A flexible arm controller which uses end of arm motion measurements, but only joint actuators has been numerically and experimentally studied and found to give good rigid body control with significant reduction in end of arm vibrations.**

ACKNOWLEDGEMENTS

The work described was based on the Ph.D. dissertation research of Ye-Chen Pan (co-advisors: A.G. Ulsoy and R.A. Scott) and Nabil Chalhoub (advisor: A.G. Ulsoy). The experimental studies were done with the assistance of Steve Culp and Rob Giles.

M

A. Galip Ulsoy

**Mechanical Engineering and Applied Mechanics
College of Engineering
University of Michigan**

REFERENCES

(available upon request from A.G. Ulsoy)

- *Dynamics of Flexible Mechanisms with Prismatic Joints*, Ye-Chen Pan, Ph.D. Dissertation, Mechanical Engineering and Applied Mechanics, University of Michigan, Ann Arbor, Michigan, April 1988.
- "Dynamic Modeling and Simulation of Flexible Robots with Prismatic Joints, Part I: Modeling and Solution Method," Y.C. Pan, R.A. Scott, and A.G. Ulsoy, (in preparation).
- "Dynamic Modeling and Simulation of Flexible Robots with Prismatic Joints, Part II: Experimental Validation and Numerical results," Y.C. Pan, A.G. Ulsoy, and R.A. Scott, (in preparation).
- *Control of a Leadscrew Driven Flexible Robot Arm*, Nabil G. Chalhoub, Ph.D. Dissertation, Mechanical Engineering and Applied Mechanics, University of Michigan, Ann Arbor, Michigan, June 1986.
- "Dynamic Simulation of a Leadscrew Driven Flexible Robot Arm and Controller," N.G. Chalhoub and A.G. Ulsoy, *ASME Journal of Dynamic Systems, Measurement and Control*, Vol. 108, No. 2, June 1986, pp 119-126.
- "Control of a Flexible Robot Arm: Experimental and Theoretical Results", N.G. Chalhoub, and A.G. Ulsoy, *ASME Journal of Dynamic Systems, Measurement, and Control*, Vol. 109, No. 4, December 1987, pp 299-309.
- "Dynamic Modeling of a Self-Locking Leadscrew and Its Implications in Robotics," N.G. Chalhoub and A.G. Ulsoy, *ASME Journal of Dynamic Systems, Measurement and Control* (submitted).